Biochimica et Biophysica Acta, 333 (1974) 261–277

BBA 46682

CHARACTERIZATION OF PRIMARY REACTANTS IN BACTERIAL PHOTOSYNTHESIS

II. KINETIC STUDIES OF THE LIGHT-INDUCED EPR SIGNAL ($g = 2.0026$) AND THE OPTICAL ABSORBANCE CHANGES AT CRYOGENIC TEMPERATURES

JAMES D. McELROY*, DAVID C. MAUZERALL**, and GEORGE FEHER***

University of California, San Diego, La Jolla, Calif. 92037 (U.S.A.)

(Received May 7th, 1973)
(Revised manuscript received October 22nd, 1973)

SUMMARY

We have shown that the rise and decay kinetics of the light-induced EPR signal are identical to the kinetics of the optical changes at 80 °K. This identity provides independent evidence that the EPR signal is due to the oxidized primary electron donor which is bacteriochlorophyll. The EPR and optical changes could be described by a model photochemical reaction scheme that takes into account spin-lattice relaxation. The optical decay rate was found to be temperature independent between 1.5 and 80 °K and to obey approximately first order kinetics. These results are consistent with the hypothesis that the charge recombination occurs via tunneling through a potential barrier. The decay constants at these temperatures were found to be the same for different bacterial species and strains. No differences were found between purified reaction centers of *R. spheroides* R-26 and whole cells. Reaction centers treated with sodium dodecylsulfate or urea were still photochemically active but showed a markedly different kinetic behavior. The decay constant may, therefore, serve as a probe to investigate the molecular environment of the primary reactants.

INTRODUCTION

Light quanta absorbed by the photosynthetic apparatus of both green plants and bacteria produce changes in its optical spectrum and gives rise to a narrow EPR signal at $g = 2.0026$. A great deal of work has been done on these two phenomena since their original discovery by Duysens [1, 2] and Commoner et al. [3]. The body

Abbreviations: P_{865}, specialized bacteriochlorophyll; $A_{\lambda}^{1\,cm}$, optical absorbance at wavelength λ for 1-cm path length.

* Present address: Bell Telephone Laboratories, Murray Hill, N.J. 07974, U.S.A.
** Present address: The Rockefeller University, New York, N.Y. 10021, U.S.A.
*** To whom correspondence should be addressed.

of knowledge acquired from these studies provides the main evidence for the identity of the primary electron donor in photosynthesis.

It is now generally accepted that the primary electron donor in bacterial photosynthesis is a bacteriochlorophyll molecule (chlorophyll molecule for green plants) or an aggregate of such molecules*. In the first part of this work we obtained evidence to support this identification by comparing the characteristics of the light-induced EPR signal with that obtained from a bacteriochlorophyll-free radical [6]. In the present study we investigate the kinetics of the light-induced optical and EPR changes. A detailed comparison of the kinetic results provides independent evidence for the identity of the donor. Several authors have studied the kinetics at room temperature and, contrary to an earlier report [7], have found identical kinetics for both the light-induced optical and EPR changes [8, 9]. Although room temperature studies have the general advantage of providing an environment that approximates physiological conditions, one cannot preclude the possibility that a nonprimary rate-limiting step has been measured (e.g. a diffusion process or a later step in the electron transfer chain). To avoid this difficulty, we have compared the kinetic behavior of the light-induced optical and EPR changes at cryogenic temperarures (1.5–80 °K) at which ordinary chemical or diffusion processes do not occur. A brief account of this work was presented earlier [10].

One of the requirements of an efficient photosynthetic process is the stabilization of the primary oxidation–reduction pair for a time long enough to allow efficient electron transfer. The mechanism of this charge separation is not understood at present. We have approached this problem by studying the decay kinetics (i.e. the lifetime of the oxidation–reduction couple) in the temperature range between 1.5 and 80 °K.

Recent advances in the understanding of the primary photochemical events have come from experiments utilizing active subchromatophore particles called reaction centers [11]. In view of the extensive purification procedures used in obtaining these particles [12–17], one may question the extent that the primary reactants have maintained their in vivo configuration. A necessary condition for this to be the case is that the kinetic behavior observed in reaction centers be the same as observed in intact cells. We have compared in this work the optical decay kinetics of different preparations obtained from several bacterial strains.

The kinetic parameters were obtained from the observed time dependence of the EPR and optical absorbance changes with the aid of a simple model that describes the photochemical process. Several experiments were performed to show the validity of the model by comparing its theoretical predictions with the observed light-induced changes.

MATERIALS AND METHODS

Bacteria, chromatophores, reaction centers

Rhodopseudomonas spheroides strain 2.4.1 and its blue-gree mutant R-26 (obtained from R. K. and B. J. Clayton), *Rhodospirillum rubrum* strain 1 and its blue-green mutant G-9 (obtained from M. D. Kamen's group) were grown in modified

* It has recently been shown that the unpaired electron is shared between two bacteriochlorophyll molecules [4, 5].

Hutner medium [18]. Inocula were obtained from single colonies of cells which were grown in the dark on agar plates. *Chromatium* was cultured heterotrophically according to Cusanovich [19]. Cultures were grown in 1-l prescription flasks placed in an illuminated constant temperature water bath, as previously described [6]. Cells were harvested by centrifugation and washed twice in 0.01 M Tris–HCl buffer, pH 8.0, to remove inorganic crystals and traces of medium.

Chromatophores from *R. spheroides* R-26 were prepared as previously described (see steps 1–4 of ref. 14). Reaction centers were obtained from this preparation by a modification due to Okamura et al. [47] of an earlier purification procedure utilizing the detergent lauryl dimethylamineoxide [14, 15].

EPR and optical samples

Samples of whole cells (washed twice) and chromatophores were suspended in 0.01 M Tris–HCl, pH 8.0, 50 % (v/v) glycerol. Reaction centers were suspended in the same buffer with the addition of 0.1 % (w/v) lauryl dimethylamineoxide. The sample concentration was adjusted to give an absorbance, $A^{1\,cm}_{800\,nm} = 2$ for reaction centers and about one half that value for whole cells and chromatophores. The optically flat quartz cuvette had dimensions 9 mm × 20 mm and an optical path length of 1 mm. The cuvette could be inserted into the microwave cavity and was used in those experiments in which a critical comparison between the optical and EPR kinetics was sought. An alternate EPR cuvette that gave a higher signal-to-noise ratio was a quartz tube with an internal diameter of 8 mm. Both types of cuvettes were fitted with calibrated resistance thermometers. The EPR and optical cuvettes were filled and left in the dark for 1 h and then lowered into liquid helium or liquid nitrogen.

Optical measurements

A single-beam spectrophotometer with provisions for cross-illumination with actinic light was used. The sample (thickness 1 mm) was positioned at the intersection of the measuring and actinic light beams at an angle of 45°. Measuring light from a Cary 14 monochromator passed through the sample and onto the photodetector which was protected from the actinic light by narrow-band interference filters. The spectrophotometer included an optical dewar (J. F. Scanlon, Inc., Whittier, Calif.) suitable for use at liquid helium temperatures. The temperature of the sample was monitored by a calibrated carbon resistance thermometer imbedded in the sample material. Temperatures in the range of 1.5–4.2 °K were reached by immersing the sample in liquid helium and reducing the pressure above the helium to the desired value. Temperatures in the range of 5–80 °K were obtained by dropping the liquid helium level below the sample and adjusting the heat input to the sample to yield the desired temperature. The maximum actinic light intensity used was approx. 30 mW/cm^2, as measured with a YSI model 65 radiometer. The heating of the sample at this light intensity was less than 20 millidegrees K at 1.5 °K.

The photomultiplier tube (RCA 7102) was mounted in a housing (Pacific Photometric, Inc.) cooled by solid CO_2. The anode of the photomultiplier was connected directly to the summing junction of a stable operational amplifier (Analog Devices 147C) which served as a current-to-voltage converter. The intensity of the measuring beam was held below 10 μW/cm^2. Photomultiplier currents of less than 10^{-7} A were used; the linearity of the response of the spectrophotometer was estab-

lished with calibrated neutral density filters. The time constant of the spectrophotometer was 0.1 ms. The signal-to-noise ratio of the spectrophotometer was increased by averaging repetitive scans with a Computer of Average Transients (CAT 1000, Technical Instruments Corp.).

The actinic light source consisted of a quartz iodine lamp (Sylvania DWY, 625 W) which was focused onto the plane of a rotating vane driven by a 90° stepping motor (Tormax 90, IMN Magnetic, Inc.). The opening and closing of the shutter were controlled by Tektronix pulsers (Models 162 and 163) triggered by the averaging computer. Light pulses of programmable duration (12 ms–10 s) with linear rise and decay complete within 0.7 ms were obtained. Lenses were used to provide uniform illumination over the relevant part of the sample. The maximum light intensity obtained at the sample position was about 30 mW/cm^2. The same actinic light source was used in the EPR experiments. In those experiments in which a better time resolution was required, a 3-μs flash (General Radio Strobotac No. 1531A) was used.

EPR measurements

A 9-GHz superheterodyne spectrometer of local design was used [20]. Magnetic field modulation (100 kHz) produced the usual derivative spectrum at the output of the spectrometer with a minimum time constant ($1/e$ rise time) of 0.2 ms. The faster magnetic relaxation rates encountered at higher temperatures were measured by the boxcar method of Isaacson [22].

The temperature dependence of the paramagnetic susceptibility χ'' was obtained from the signal amplitude S by the relation

$$\chi'' \propto \frac{S\Delta H^2}{GQ\sqrt{P}} \tag{1}$$

where G is the total spectrometer gain, ΔH is the line width, Q the quality factor of the cavity and P the microwave power. This method was checked by determining the temperature dependence of χ'' for a single crystal of $CuSO_4 \cdot 5H_2O$ (approx. 3 mg) which was in thermal contact with the frozen reaction center sample through a thin layer of silicone grease. The temperature dependence obtained was in agreement with published results which, in the liquid helium temperature range, are described by a Curie–Weiss law (see for example ref. 23) with a Curie temperature of -0.6 °K [24]. The temperature of the sample could be varied and monitored in the range of 1.5–80 °K as described in the previous section.

The magnetic relaxation experiments were carried out by switching simultaneously the level of the microwave power and the sensitivity of the spectrometer with a matched pair of PIN diodes (Hewlet Packard 8735A). With this arrangement the observed EPR signal was directly proportional to the population difference of the Zeeman levels, i.e. the susceptibility χ''.

Relaxation measurements and analysis of data

A general method of obtaining kinetic parameters of a system is to apply a sudden perturbation and to monitor the time dependence of the equilibration (i.e. relaxation) process [25–27]. In the present work we have used three distinct types of relaxation measurements which differ from each other in the nature of the applied

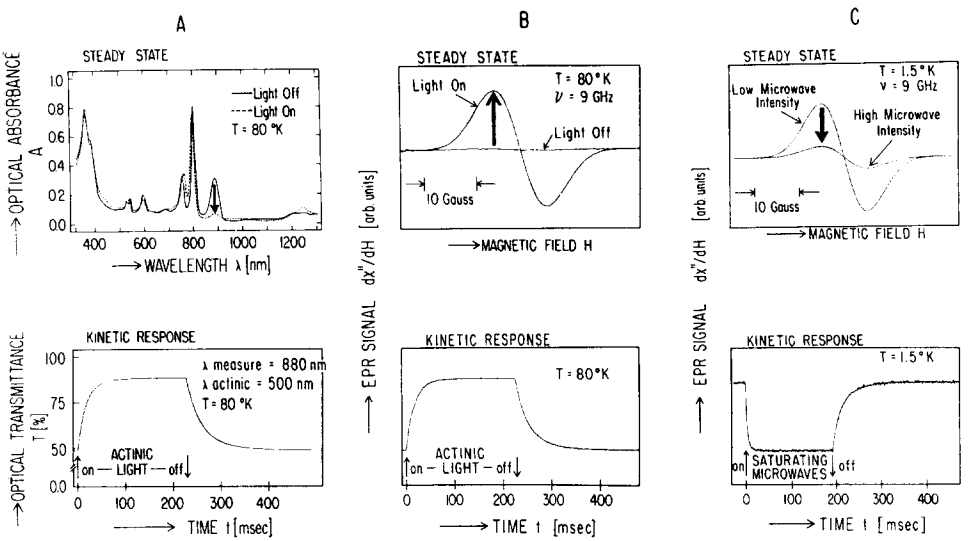

Fig. 1. Three types of relaxation measurements performed on reaction centers of *R. spheroides* R-26. Top traces show the steady state behavior; bottom traces the kinetic response to a perturbation at the position of the arrows. (A) The steady-state optical spectrum with and without actinic light was recorded with the Cary 14 R spectrophotometer in the I.R. II and I.R. I mode, respectively. The kinetic response was obtained with an actinic light intensity of approx. 30 mW/cm^2 in a wavelength band of 50 nm centered at 500 nm. The wavelength of the measuring light was 880 nm (see arrow). (B) Light-induced EPR signal obtained with the same actinic light as in A. The kinetic response was obtained by setting the magnetic field to a value corresponding to the peak of the signal. (C) Recovery from microwave saturation of the EPR signal obtained with constant actinic light.

perturbation and/or the physical parameters that are being monitored. The three types of measurements are: (A) Optical absorbance changes induced by actinic light; (B) Amplitude changes of the EPR signal induced by actinic light; (C) Amplitude changes of the EPR signal induced by a saturating microwave pulse. Typical experimental traces of the three types of measurements are shown in Figs 1A, B, and C. The top panel of each of these figures shows the steady state behavior of the system with and without the applied perturbation. The "heavy" arrow indicates the position on the abscissa (wavelength or magnetic field) at which the response to the perturbation is observed. The time dependence of the amplitude of the signal at the position of the arrow contains the desired information and is shown in the bottom part of the figure.

The changes in transmission (ΔT) recorded by the kinetic spectrophotometer were converted into absorbance changes (ΔA), using the expression:

$$\Delta A = -\log_{10}\left(1+\frac{\Delta T}{T}\right) \tag{2}$$

where T is the initial value of the transmission. From the changes of the absorbance and the amplitude of the EPR signal, the kinetic parameters were obtained by fitting their time dependence with exponential functions. We found that the best fit was obtained by assuming a fast principal component and a minor component with slower

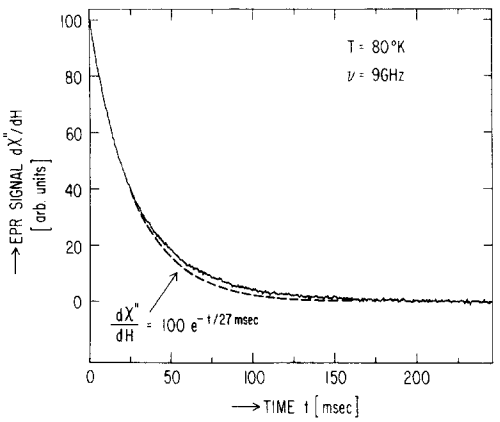

Fig. 2. Decay of the EPR signal in reaction centers of *R. spheroides* R-26 after removal of actinic light. The dotted line is a theoretical (exponential) fit with a single decay time constant of 27 ms. A similar deviation from a single exponential was observed in the kinetic behavior of the light-induced absorbance changes.

kinetics. The same biphasic kinetics were observed in both optical and EPR experiments. An example of the deviation from a single exponential is shown for the EPR decay in Fig. 2. Small deviations from an exponential have also been reported in chromatophores at room temperatures [8]. In view of the small value of the slow component, a systematic decomposition of the kinetic traces did not seem warranted. Accordingly, all the light-induced optical (and EPR) kinetics reported here are characterized by the exponential fitted to the fast principal component only.

EXPERIMENTAL RESULTS

Optical decay kinetics of different preparations from R. spheroides R-26

Before investigating the details of the kinetic behavior of reaction centers, we wished to determine whether or not their low-temperature kinetics are identical to those of the photosynthetic apparatus in the intact organism. Accordingly, we compared the optical decay kinetics of whole cells, chromatophores, and reaction centers; the latter remained either untreated or were treated with a mixture of sodium dodecyl sulfate and lauryl dimethylamineoxide [28] or 6 M urea. The results presented in Table I show that purified reaction centers in 0.1 % lauryl dimethylamineoxide exhibit the same optical decay kinetics as whole cells. Thus, as judged from the kinetic behavior, the reaction centers preserve the integrity of the primary photochemical apparatus. When the reaction centers were subjected to denaturing agents (e.g. sodium dodecylsulfate, urea), their photochemical activity was preserved, but their kinetic parameters changed drastically, indicating that the protein–bacteriochlorophyll complex had undergone a structural change.

Optical decay kinetics of different bacterial species

Since we are working with a carotenoidless mutant of *R. spheroides*, it was of interest to establish the generality of these findings by comparing the kinetic behavior

of the mutant with its wild type and with other bacterial species. Table II shows the close similarity of the optical decay constant among the species examined. Thus, having established the generality of the kinetic results obtained from reaction centers of *R. spheroides* R-26, we turn now to explore the effects of other parameters on the decay kinetics.

TABLE I

OPTICAL DECAY KINETICS OF WHOLE CELLS, CHROMATOPHORES, AND REACTION CENTERS OF *R. SPHEROIDES*, R-26

Whole cells and chromatophores were suspended in 50 % glycerol, 0.05 M Tris, pH 8.0, to give $A_{800\ nm}$ of approx. 0.1 (1 mm path). The presence of glycerol did not affect the kinetic behavior. It was used to insure the formation of a transparent glassy matrix at low temperatures. Reaction centers, unless otherwise specified, were suspended in the same buffer to give $A_{800\ nm}$ of approx. 0.2 (1 mm path) at room temperature. Reaction centers which were exposed to 6 M urea for 4 h at 20 °C in the dark had an absorbance $A_{800\ nm}$ of approx. 1.0 (1 mm path). The decay of the optical change at 795 nm was monitored at a sample temperature of 80 °K. The wavelength of the actinic illumination was 900 nm. The measuring beam intensity was approx. 5 $\mu W/cm^2$.

Preparation	1/e decay time	Treatment
Whole cells	30 ± 3 ms	No detergent
Chromatophores	32 ± 3 ms	No detergent
Reaction centers	29 ± 2 ms	0.1 % lauryl dimethyl-amineoxide
Reaction centers	52 %, 28 ms, 48 %, 93 ms	6 M urea, 0.1 % lauryl dimethylamineoxide, $t = 4$ h
Reaction centers [28]	60 %, 260 ms, 40 %, 1.8 s	0.1 % sodium dodecyl-sulfate, 0.02 % lauryl dimethylamineoxide

TABLE II

OPTICAL DECAY KINETICS OF SEVERAL SPECIES OF PHOTOSYNTHETIC BACTERIA

Whole cells were suspended in 50 % glycerol, 50 % 0.01 M buffer (either glycylglycine, pH 7.8, or Tris–HCl, pH 8.0) under aerobic conditions to give $A_{800\ nm}$ of approx. 0.1 (1 mm path). Sample temperature was 2.1 °K. The decay of the absorbance change was monitored at 795 nm. Other experimental conditions those of Table I.

Species	1/e decay time (ms)
R. spheroides, St. R-26	30 ± 3
R. spheroides, St. 2.4.1	31 ± 3
R. rubrum, St. 1	24 ± 3
R. rubrum, St. G-9	23 ± 3
Chromatium, St. D	27 ± 3

Temperature dependence of optical decay kinetics

One of the striking earlier findings was the identical decay rate of the optical changes at 1.7 and 77 °K [10]. We have repeated and extended this work to cover intermediate temperatures. The results are summarized in Fig. 3. The decay rate remains essentially unchanged in the temperature range of 1.6–80 °K. The process of charge recombination cannot, therefore, be a thermally activated process that would predict an $\exp(-\Delta E/kT)$ dependence of the rate constant. From the experimental uncertainty of the measurements (see error bars in Fig. 3), we estimate that ΔE must be less than 0.2 °K (0.4 cal/mole).

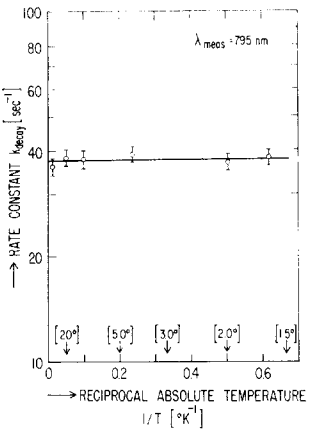

Fig. 3. Kinetics of light-induced optical changes as a function of temperature in reaction centers of *R. spheroides* R-26. The upper limit on the activation energy of the decay reaction is approx. 0.4 cal/mole. Experimental conditions same as described in Table I.

Optical decay kinetics at different wavelengths

We have investigated the optical decay kinetics at the following wavelengths: 1242, 880, 802, 795, 600, 443 nm. These correspond to the peaks of the low-temperature "light–dark" difference spectrum. We have found that the decay kinetics are, within experimental error ($\pm 7\,\%$), the same for all wavelengths investigated. One can choose, therefore, any convenient wavelength to study the kinetics of the light-induced changes.

Comparison of the light-induced optical and EPR changes

If the light-induced optical changes and the EPR signal arise from the same chemical species, their kinetics should be identical at a temperature at which the spin-lattice relaxation rate is fast compared to the other observed rates (see Appendix). This condition is satisfied at 80 °K; we chose, therefore, this temperature to perform a detailed comparison of the optical and EPR kinetics.

The optical and EPR rise kinetics have been presented earlier [10]. In these experiments, the same sample and the same actinic light intensity were used for both the optical and EPR measurements. We found that within experimental error identical rise times were obtained for both sets of measurements. Furthermore, we found that within our time resolution of 0.3 ms, there was no lag between the actinic light flash and the appearance of the EPR and optical absorbance changes.

The ratio of the decay kinetics were obtained on the same sample at 80 °K and were found to be

$$\frac{k_d(\Delta A)}{k_d(\mathrm{EPR})} = 1.06 \pm 0.10$$

Test of the photochemical model

The photochemical model (see Appendix) predicts that the amplitude ΔA of the optical absorbance changes with continuous illumination saturates with increasing light intensity. Since k_i is proportional to the actinic light intensity and k_d is a constant we can rewrite Eqn 17 in terms of the normalized reciprocal actinic light intensity I_0/I

$$\frac{1}{\Delta A} = \left(\frac{1}{\Delta A_{max}}\right)\left(1 + \frac{I_0}{I}\right) \tag{3}$$

where I_0 is a constant, depending on the light source.

In Fig. 4A, we have plotted $1/A$ against I_0/I. The good fit of the experimental data to a straight line over a factor of 10 in reciprocal light intensity demonstrates the validity of Eqn 17. The intercept of the straight line with the ordinate gives the value for the maximum absorbance change which occurs when all molecules are in the excited state.

The kinetic behavior of the optical absorbance changes with step-function illumination is described by Eqn 18. The experimentally determined rise and decay rate constants are plotted against light intensity in Fig. 4B. We note that the decay kinetics are independent of light intensity as predicted by the model ($k_{decay} = k_d$).

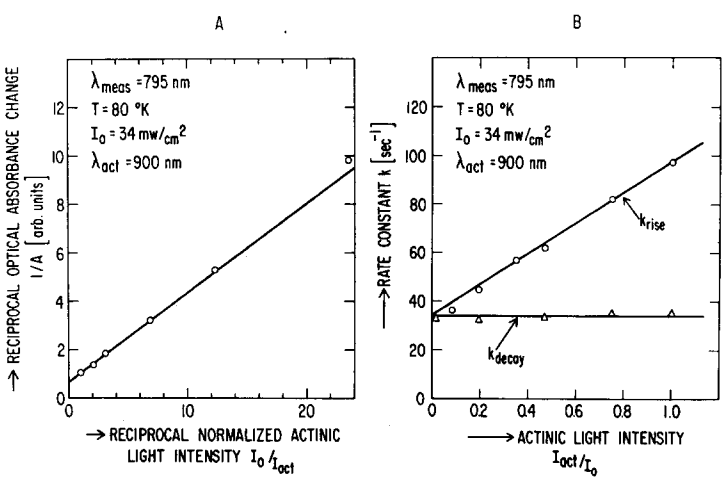

Fig. 4. Light-induced optical absorbance changes in reaction centers of *R. spheroides* R-26, suspended in 0.01 M Tris–HCl, pH 8.0, 0.1 % lauryl dimethylamineoxide, 50 % glycerol. $A_{800\,nm} = 0.1$ (1 mm path) at room temperature. Other conditions as described in Table I. (A) Absorbance changes for different actinic light intensities. Straight line predicted by Eqn 17. (B) Rise and decay kinetics of the absorbance changes at different actinic light intensities. The decay kinetics are expected to be independent of, and the rise kinetics proportional to, the light intensity (Eqn 18).

The rate constant of the rise kinetics is a linear function of the actinic light intensity approaching at low light intensity the decay rate constant as predicted by Eqn 18.

In the case of the EPR changes an added complexity arises from the spin-lattice relaxation rate k_1. Its value may be obtained from the recovery of the EPR signal from microwave saturation. The recovery rate k_{rec} is given by $k_d + k_1$ (Eqn 14). At low temperatures $k_1 \ll k_d$ ahd $k_{rec} = k_d$, whereas at high temperatures $k_1 \gg k_d$ and $k_{rec} = k_1$. These predictions are borne out by the experimentally determined recovery rates at different temperatures (Fig. 5A). When the reaction centers are illuminated while being cooled, the free radical signal is "frozen in", i.e. it does not decay. At 2 °K, we found k_1 in the frozen-in radical to be approx. 0.15 s^{-1} which is two orders of magnitude smaller than the recovery rate k_{rec} of the light-induced radical.

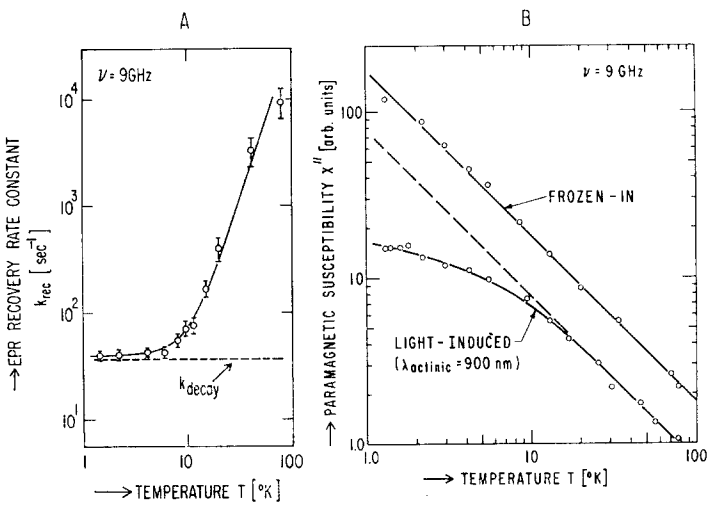

Fig. 5. Consequences of the competition between the spin-lattice relaxation rates and the lifetime of the free radical P_{865}^+ in reaction centers of *R. spheroides* R-26. Sample conditions same as in Fig. 4. (A) EPR recovery rate from microwave power saturation as a function of temperature (see Fig. 1C). The photochemical model predicts (Eqn 12) that at low temperatures the recovery rate constant should approach k_d as indeed is found. (B) Temperature dependence of the microwave susceptibility of the light-induced and frozen-in radical. The latter was obtained by illuminating the sample with actinic light (150 W Xenon lamp filtered by 6 cm water and a Corning C.S. 2-64 filter, light intensity 100–150 mW/cm²) while freezing it with a stream of liquid nitrogen. The deviation from the straight line (Curie law) of the light-induced radical is predicted from the model by Eqn 13. Care was taken to avoid microwave power saturation of the EPR signal.

The competition between magnetic relaxation and the lifetime of the radical causes the temperature dependence of the magnetic susceptibility to deviate from the Curie law. Fig. 5B shows this deviation; the dotted line represents the Curie law, and the solid line is a fit through the experimental data using Eqn 13 and assuming k_1 to be proportional to T. The susceptibility of the frozen-in radical obeys the Curie law as expected (Fig. 5B). The quantitative agreement between the results obtained from the susceptibility and recovery rate measurements is not perfect. For instance, the value of k_1 at 3 °K, estimated from the susceptibility measurements (Fig. 5B),

predicts a recovery rate constant a factor of two larger than the observed value shown in Fig. 5A.

At lower temperatures, Eqn 15 of the model predicts that the EPR changes with step-function illumination will become nonexponential and slower than that of the corresponding optical changes. The experimental decays are plotted on a logarithmic scale and compared in Fig. 6 with the theoretical predictions. At 80 °K, $k_1 \gg k_d$ and a straight line is obtained as expected from theory. At 1.5 °K, the observed EPR decay (Fig. 6A) has the general shape of the predicted curve for $k_1 = k_d$ (Fig. 6B).

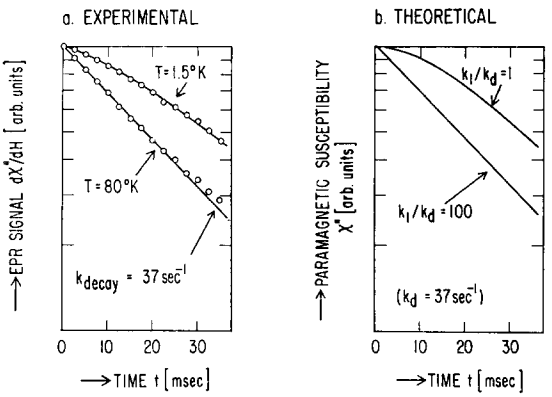

Fig. 6. Comparison of the experimental and theoretical behavior of the light-induced EPR signal in reaction centers of *R. spheroides* R-26. Sample conditions same as in Fig. 4. (A) The experimentally observed decay kinetics are replotted an a logarithmic scale for the high (80 °K) and low (1.5 °K) temperature case. The deviation from a straight line for the high temperature case is due to a small admixture of a slower decaying component, as discussed in text (see also Fig. 2). (B) The theoretical curves given by Eqn 15 with k_1/k_d as an adjustable parameter. Note the slower, nonexponential kinetics for the low temperature case.

DISCUSSION AND CONCLUSIONS

We have shown that both the rise and decay kinetics of the light-induced EPR signal are identical to those of the optical changes at 80 °K. The optical changes have previously been shown to be associated with the photo-oxidation of the specialized bacteriochlorophyll P_{865} [29] and to constitute the primary photochemical step [30]. In a separate study we have shown that the EPR signal is due to a bacteriochlorophyll radical [6]. The identity of the optical and EPR kinetics, therefore, provides independent evidence that the EPR signal arises from the oxidized primary electron donor (i.e. $BChl^+$, or more likely, $BChl_2^+$ [4, 5]). However, we cannot exclude by these kinetic measurements alone the existence of intermediates that decay in a time short in comparison to our resolution time of approx. 10^{-4} s.

The first experiments that demonstrated photochemical reversibility at cryogenic temperatures were performed by Sogo, et al. [31] and Arnold and Clayton [32]. The former showed that the light-induced EPR signal in chromatophores of *Chromatium* had a decay time of less than one second at −140 °C. Arnold and Clayton described their decay data with second order kinetics. Parson found with chromato-

phores of *R. rubrum* [33] a first order kinetic behavior of approximately the same magnitude as the ones reported here. He observed, however, a small but significant linear temperature dependence of k_d in the temperature region between 38 and 150 °K. In our studies on reaction centers of *R. spheroides* R-26 we found that : (1) The EPR and optical changes follow first order kinetics to a good approximation, and (2) The optical decay time is temperature independent between 1.5 and 80 °K.

A simple mechanism that can give rise to a temperature independent first order decay over such a large (50-fold) temperature region is tunneling through a potential barrier. Such a mechanism has been proposed earlier by Chance and coworkers [34, 35] in connection with cytochrome oxidation. The tunneling rate constant (i.e. decay rate k_d in our case) for a one-dimensional square barrier is given by [36]:

$$k_d = \frac{8E^2(V-E)}{\pi\hbar V^2} e^{-2d[2m(V-E)]^{\frac{1}{2}}/\hbar} \tag{4}$$

where $\hbar$ is Planck's constant divided by 2π, m the mass of the electron, V the height of the barrier, E the energy of the electron and d the width of the potential barrier. Assuming, for an order of magnitude calculation $\frac{1}{2}V = E \approx 1$ eV then for the observed decay time of 30 ms, one obtains from Eqn 4 a potential barrier width of 30 Å. This is not an unreasonable value for the donor–acceptor distance; there exists experimental evidence for electron transfer over 20 Å from excited states of metalloporphyrins to acceptors in solutions [37].

A remarkable consequence of tunneling is the extreme sensitivity of the tunneling time on the width of the barrier. A 3 % change in d (i.e. 1 Å) would approximately triple the value of k_d. A 50 % increase in d (or an approximate doubling of $(V-E)$) would result in a decay time of about 10^5 s (approximately one day!). This, perhaps, could account for the fact that in plants the primary photoact is only partially reversible at low temperatures [38].

It should be kept in mind, however, that the temperature independence of k_d is consistent with, but does not constitute a proof of, the tunneling hypothesis. Another temperature independent mechanism of a different nature could, for example, involve the decay of a metastable triplet state. Although triplet states in reaction centers have been recently observed [39, 40], their function in photosynthesis is not clear. Furthermore, we see no way to incorporate such states in our reaction scheme compatible with our experimental findings. It should be also noted that at higher temperatures ($T > 80$ °K) thermally activated processes as well as changes in the tunneling distance and/or barrier height (due to dimensional changes) are expected to affect the decay rate.

Since the decay rate k_d involves the recombination of two spatially separated charges, it is likely that its value will reflect structural details of the photosynthetic protein–chlorophyll complex. Accordingly, we have explored the effect of a variety of purification procedures and chemical treatments on the optical decay kinetics. We found that the low temperature optical decay kinetics of purified reaction centers in 0.1 % lauryl dimethylamineoxide are identical to the ones observed in whole cells. Treatment of the reaction centers with more potent reagents (urea, sodium dodecylsulfate) changed the decay kinetics significantly (see Table I) as would be expected from an altered three-dimensional configuration.

A phenomenon related to the above discussion is the "freezing in" of P^+ (i.e. the EPR signal) when the reaction centers are illuminated while being cooled to cryogenic temperatures. There are at least two possible explanations of this effect. (1) The primary acceptor is re-oxidized, i.e. the electron is removed from $P^+ \cdot X^-$. Consequently, at low temperatures, the complex $P^+ \cdot X$ is frozen in; since P^+ can no longer receive an electron from X; it remains charged and stable. (2) A conformational change of the reaction centers occurs during illumination at room temperature. If this conformational change is frozen in, the recombination time may become too long to be observed. At present, it is not possible to decide between these two alternatives.

One probe that shows promise in the determination of the donor–acceptor distance is the spin-lattice relaxation rate. If the primary acceptor is iron, as has been postulated [14, 41–43], it is likely that its relaxation rate will be faster than that of the bacteriochlorophyll radical, P^+. In this case, the spin of P^+ may relax via the iron spin, a process whose rate constants will depend on the distance between the two primary reactants. A quantitative utilization of this effect awaits the further characterization of X^-. Work along these lines is in progress and will be published in a future paper of this series.

The kinetic parameters reported here were obtained from the observed time dependence of the light-induced EPR and optical absorbance changes with the aid of a simple model that takes into account the effect of the electron spin-lattice relaxation time (see Appendix). We have tested the predictions of this model in the temperature range between 1.5 and 80 °K. At 80 °K, complete quantitative agreement was obtained for both the light-induced optical and EPR changes. The lag between the onset of the actinic light and the EPR signal which had been reported to be 2–3 ms [44] was not confirmed. Within our time resolution of 0.2 ms, no lag was observed. These findings are consistent with those reported by Bolton et al. [45] with an instrumental resolution of 1 ms.

At the lower temperatures ($T < 20$ °K), the qualitative behavior predicted by the model was borne out (see Figs 4–6). However, some quantitative discrepancies, for example, between the observed recovery rate (Fig. 5A) and susceptibility (Fig. 5B) remained. These discrepancies may be associated with the observed deviation of the kinetics from a single exponential (see Fig. 4) and probably indicate that the samples are not completely homogenous with respect to the detailed environment of the primary reactant. The model does not take into account such inhomogeneities which may account for the observed quantitative discrepancies. However, all of the conclusions arrived at in this work are based on either the high temperature (80 °K) optical and EPR changes or the low temperature optical data for which the model accounts quantitatively.

APPENDIX

Theoretical model of the photochemical reaction scheme

Light-induced EPR signal. Light causes an electron to be transferred from P_{865} to the primary electron acceptor producing a radical state $P_{865}{}^+$. In an EPR experiment, the ground state of $P_{865}{}^+$ is split by an external magnetic field into two Zeeman levels (Fig. 7) assumed to be populated with equal probability by the actinic

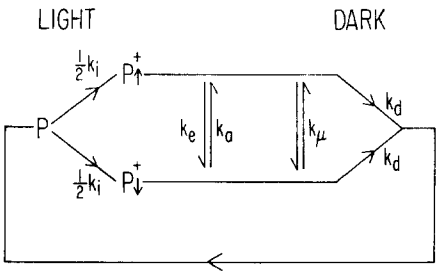

Fig. 7. Model photochemical reaction scheme used to derive the light-induced EPR kinetics and the optical absorbance changes. $P^+\uparrow$ and $P^+\downarrow$ are the free radical concentrations in the two Zeeman levels. k_e, k_a, and k_μ are the rates at which spin transitions are being induced by the lattice vibrations and microwave field, respectively. The electron acceptor has been omitted for simplicity.

light. Let P, $P^+\uparrow$ and $P^+\downarrow$ be the concentrations of P_{865} and $P_{865}{}^+$ in their respective spin states ($P^+ = P^+\uparrow + P^+\downarrow$) and P^0 be the total concentration of molecules ($P^0 = P + P^+$); k_i is the rate constant with which P^+ is created and k_d, that of its decay; k_μ is the rate constant with which the microwave magnetic field induces transitions; k_e and k_a are the rate constants with which lattice vibrations are emitted or absorbed by the spin system with resulting change in the spin state. The rate equations describing the scheme of Fig. 7 are given by:

$$\frac{dP}{dt} = -k_i P + k_d(P^+\uparrow + P^+\downarrow) \tag{5}$$

$$\frac{dP^+\downarrow}{dt} = \tfrac{1}{2}k_i P - k_d P^+\downarrow - (k_a + k_\mu)P^+\downarrow + (k_e + k_\mu)P^+\uparrow \tag{6}$$

$$\frac{dP^+\uparrow}{dt} = \tfrac{1}{2}k_i P - k_d P^+\uparrow - (k_e + k_\mu)P^+\uparrow + (k_a + k_\mu)P^+\downarrow \tag{7}$$

The EPR signal is proportional to the difference in population n between the two Zeeman levels. Subtracting Eqn 7 from 6, one obtains:

$$\frac{d(P^+\downarrow - P^+\uparrow)}{dt} = \frac{dn}{dt} = -(k_1 + k_d + 2k_\mu)n + k_1 \left(\tanh \frac{h\nu}{2kT}\right) P^+ \tag{8}$$

where $h\nu$ is the Zeeman energy, k is Boltzman's constant and $k_e - k_a$ was replaced by the relation [46]:

$$k_e - k_a = k_1 \tanh \frac{h\nu}{2kT} \tag{9}$$

where $k_1 = k_e + k_a$ is the reciprocal of the spin-lattice relaxation time T_1. At low microwave power (i.e. $k_\mu \to 0$), the equilibrium population difference n_0 is given by:

$$n_0 = P^+ \tanh \frac{h\nu}{2kT} \tag{10}$$

and Eqn 8 reduces to:

$$\frac{dn}{dt} = k_1(n_0 - n) - k_d n = \frac{1}{T_1}(n_0 - n) - \frac{n}{\tau_d} \tag{11}$$

where $k_d = 1/\tau_d$. Eqns 8 and 11 differ from the usual rate equations for a spin system [46] by containing an additional term describing the decay of the radical state. Eqn 8 can be solved for two distinct cases: continuous illumination with actinic light and step-function changes in the actinic light intensity.

If the system is continuously illuminated, a steady-state concentration of P^+ radicals is formed. Let us first discuss the effect of microwave power on the EPR signal. At high microwave powers the populations of the Zeeman levels tend to be equalized (microwave saturation). When the microwave power is suddenly reduced the population difference n will start to increase from zero until the equilibrium population difference n_0 is reached. The time dependence of n after a sudden (step function) reduction in microwave power (to a non-saturating level, i.e. $k_\mu \ll k_1, k_d$) is obtained from Eqn 8

$$n(t) = \frac{k_1}{k_1 + k_d} n_0 [1 - e^{-(k_1 + k_d)t}] \tag{12}$$

This expression shows that the observed recovery rate constant is not k_1, as expected from a static spin population, but rather the sum of k_1 and k_d. At low temperatures the spin lattice relaxation $k_1 \ll k_d$ and the recovery rate of n is governed entirely by the lifetime of the free radical. Under these conditions the EPR signal from the light-induced free radicals saturates at higher microwave powers than it would if the same free radicals were "frozen in" at low temperatures ($k_d = 0$).

The temperature dependence of the magnetic susceptibility (i.e. EPR signal) is proportional to the population difference $n(T)$. For low microwave powers ($k_\mu \ll k_1, k_d$) the steady-state population difference $n(T)$ is obtained from Eqns 10 and 12 by letting $t \to \infty$

$$n(T) = \frac{k_1}{k_1 + k_d} P^+ \tanh \frac{h\nu}{2kT}. \tag{13}$$

In the high temperature limit (i.e. $h\nu < kT$) which is valid at $\nu = 9$ GHz for temperatures above 1 °K, Eqn 13 reduces to:

$$n(T) = \frac{1}{1 + (k_d/k_1)} \frac{P^+}{2} \frac{h\nu}{kT} \tag{14}$$

For a static spin population ($k_d = 0$), Eqn 14 predicts that the EPR signal is inversely proportional to temperature; this is the well-known Curie law. However, if k_d becomes comparable to or larger than k_1, the light-induced EPR signal will be reduced by the factor $[1 + k_d/k_1]^{-1}$, where k_1 is temperature dependent.

For step-function changes in the actinic light intensity, one obtains from Eqns 5 and 11 for the kinetics of the population difference in the absence of microwave saturation ($k_\mu \ll k_1, k_d$):

$$n(t) = \frac{n_0}{1+(k_d/k_1)} \cdot \begin{cases} 1-e^{-(k_d+k_i)t}\left[\dfrac{(k_d+k_1)-(k_d+k_i)e^{-(k_1-k_i)t}}{k_1-k_i}\right] & \text{LIGHT ON} \\ e^{-k_d t}\left[\dfrac{(k_d+k_1)-k_d e^{-k_1 t}}{k_1}\right] & \text{LIGHT OFF} \end{cases} \tag{15}$$

The above relations simplify considerably when the spin lattice relaxation rate k_1 is larger than either k_d or k_i. Under these conditions ($k_1 \gg k_d, k_i$) Eqn 15 reduces to:

$$n(t) = n_0 \cdot \begin{cases} 1-e^{-(k_d+k_i)t} & \text{LIGHT ON} \\ e^{-k_d t} & \text{LIGHT OFF} \end{cases} \tag{16}$$

Light-induced absorbance changes

The kinetics of the optical changes are proportional to the concentration changes in P (i.e. $\Delta P(t)$) and are equal to $P^+(t)$. They can be obtained from Eqns 5, 6, 7 as a special case by setting $P^+ = P^+\uparrow + P\downarrow^+$.

With continuous illumination, the steady state free radical concentration is obtained by setting $dP^+/dt = 0$. The amount of bleaching ΔP is then given by:

$$\Delta P = P_0/(1+k_d/k_i) \tag{17}$$

For step-function changes in the actinic light intensity, one obtains

$$\Delta P(t) = P^+(t) = \frac{k_i P_0}{k_d+k_i} \cdot \begin{cases} 1-\exp\left[-(k_d+k_i)t\right] & \text{LIGHT ON} \\ \exp\left(-k_d t\right) & \text{LIGHT OFF} \end{cases} \tag{18}$$

The time dependence of this expression is identical to the one obtained for the kinetics of the EPR signal for the case of fast spin lattice relaxation time ($k_1 \gg k_d, k_i$) (Eqn 16).

ACKNOWLEDGMENTS

We thank R. A. Isaacson for his expert technical assistance, in particular with the measurements of the fast spin-lattice relaxation times and Mr E. Moskowitz for his assistance with several optical decay measurements. We are indebted to Drs M. D. Kamen, R. Bartsch, and M. A. Cusanovich, for gifts of inocula and for the use of some of their facilities. Dr M. Y. Okamura and Mr E. Moskowitz provided some of the reaction center material used in this work. The work was supported by grants from the National Science Foundation (GB-33340X) and the National Institutes of Health (GM-13191). J. D. M. was supported in part by a Special Fellowship (GM-44384) from the National Institute of General Medical Sciences. D. C. M. acknowledges the support of a Guggenheim Fellowship. This work was carried out in partial fulfillment of the requirements for the doctorate of J. D. M.

NOTE ADDED IN PROOF (Received December 21st, 1973)

E. Moskowitz in our laboratory has recently measured the optical kinetics of whole cells and chromatophores of *Rhodopseudomonas viridis* (sample temperature

80 °K, wavelength of measuring light 970 nm). The decay time was found to be 9 ± 1 ms which is approx. 3 times shorter than that found in the other photosynthetic bacteria (Table II). The bacteriochlorophyll of *R. viridis* is type *b* which is structurally different from bacteriochlorophyll *a* encountered in the other bacteria investigated in this work. The optical and circular dichroism spectra of *R. viridis* (Philipson and Sauer [48]) and the EPR line width (6) also differ from those observed in other bacteria.

REFERENCES

1 Duysens, L. N. M. (1952) Thesis, Utrecht, The Netherlands
2 Duysens, L. N. M., Huiskamp, W. J., Vos, I. J. and Van der Hart, M. (1956) Biochim. Biophys. Acta 19, 188–190
3 Commoner, B., Heise, J. T. and Townsend, J. (1956) Proc. Natl. Acad. Sci. U.S. 42, 710–718
4 Feher, G., Hoff, A. J., Isaacson, R. A. and McElroy, J. D. (1973) Biophys. Soc. Abstr., p. 61a
5 Norris, J. R., Druyan, M. E. and Katz, J. J. (1973) J. Am. Chem. Soc. 95, 1680–1684
6 McElroy, J. D., Feher, G. and Mauzerall, D. (1972) Biochim. Biophys. Acta 267, 363–374
7 Ruby, R. H., Kuntz, Jr., I. D. and Calvin, M. (1964) Proc. Natl. Acad. Sci. U.S. 51, 515–520
8 Loach, P. A. and Sekura, D. L. (1967) Photochem. Photobiol. 6, 381–393
9 Bolton, J. R., Clayton, R. K. and Reed, D. W. (1969) Photochem. Photobiol. 9, 209–218
10 McElroy, J. D., Feher, G. and Mauzerall, D. C. (1969) Biochim. Biophys. Acta 172, 180–183
11 Clayton, R. K. (1963) Biochim. Biophys. Acta 75, 312–323
12 Reed, D. W. and Clayton, R. K. (1968) Biochem. Biophys. Res. Commun. 30, 471–475
13 Loach, P. A., Sekura, D. L., Hadsell, R. M. and Stemer, A. (1970) Biochemistry 9, 724–733
14 Feher, G. (1971) Photochem. Photobiol. 14, 373–388
15 Clayton, R. K. and Wang, R. T. (1971) Methods Enzymol. XXIII, 696–704
16 Reiss-Husson, F. and Jolchine, G. (1972) Biochim. Biophys. Acta 256, 440–451
17 Slooten, L. (1972) Biochim. Biophys. Acta 256, 452–466
18 DeKlerk, H., Bartsch, R. G. and Kamen, M. D. (1965) Biochim. Biophys. Acta 97, 275–380
19 Cusanovich, M. A. and Kamen, M. D. (1968) Biochim. Biophys. Acta 153, 376–396
20 Feher, G. (1957) Bell Syst. Tech. J. 36, 449–484
21 McElroy, J. D. (1972), Ph. D. thesis, University of California, San Diego
22 Isaacson, R. A. (1969) J. Sci. Instr. (Ser. 2) 1, 1137–1139
23 Kittel, C. (1971) in Introduction to Solid State Physics, pp. 502–506, John Wiley and Sons, New York
24 Miedema, A. R., Van Kempen, H., Haseda, T. and Huiskamp, W. J. (1962) Physica 28, 119–130
25 Hahn, E. L. (1949) Phys. Rev. 76, 145–146
26 Weissberger, A. (1963) Techniques of Organic Chemistry, Vol. VIII, Part II, Interscience Publishers, New York
27 Kustin, K. (1969) Methods in Enzymology, Vol. XVI, Academic Press, New York
28 Feher, G., Okamura, M. Y. and McElroy, J. D. (1972) Biochim. Biophys. Acta 267, 222–226
29 Loach, P. A., Androes, G. M., Maksim, A. F. and Calvin, M. (1963) Photochem. Photobiol. 2, 443–454
30 Parson, W. W. (1968) Biochim. Biophys. Acta 153, 248–259
31 Sogo, P., Jost, M. and Calvin, M. (1959) Radiat. Res. Suppl. 1, 511–518
32 Arnold, W. and Clayton, R. K. (1960) Proc. Natl. Acad. Sci. U.S. 46, 769–776
33 Parson, W. W. (1967) Biochim. Biophys. Acta 131, 154–172
34 Chance, B., DeVault, D., Hildreth, W. W., Parson, W. W. and Nishimura, M. (1966) in Energy Conversion by the Photosynthetic Apparatus, Brookhaven Symposium in Biology, Vol. 19, pp. 115–125, BNL-Biology Department, Upton, New York
35 DeVault, D. and Chance, B. (1966) Biophys. J. 6, 825–847
36 Schiff, L. I. (1955) Quantum Mechanics, 2nd edn, pp. 94–95, McGraw-Hill, New York
37 Mauzerall, D. (1973) Ann. N.Y. Acad. Sci., 206, 483–494
38 Mayne, B. C. and Rubinstein, D. (1966) Nature 210, 734–735

39 Dutton, P. L., Leigh, J. S. and Seibert, M. (1972) Biochem. Biophys. Res. Commun. 46, 406–413,
40 Parson, W. W. and Clayton, R. K. (1973) Biophys. Soc. Abstr. p. 61
41 McElroy, J. D., Feher, G. and Mauzerall, D. C. (1970) Biophys. Soc. Abstr., p. 204a
42 Feher, G. (1970) in Electron Paramagnetic Resonance with Applications to Selected Problems in Biology, pp. 98–103, Gordon and Breach, New York
43 Leigh, J. S. and Dutton, P. L. (1972) Biochem. Biophys. Res. Commun. 46, 414–421
44 Commoner, B., Kohl, D. H. and Townsend, J. (1963) Proc. Natl. Acad. Sci. U.S. 50, 638–644
45 Bolton, J. R., Cost, K. and Frenkel, A. W. (1968) Arch. Biochem. Biophys. 126, 383–387
46 Pake, G. E. (1962) Paramagnetic Resonance, pp. 16–40, W. A. Benjamin, Inc., New York
47 Okamura, M. Y., Steiner, L. A. and Feher, G. (1974) Biochemistry, in the press
48 Philipson, K. D. and Sauer, K. (1973) Biochemistry 12, 535–539